FAILURE PREDICTION OF STRINGER STIFFENED COMPOSITE PANELS WITH IMPACT DAMAGE UNDER UNIAXIAL COMPRESSION

P. T. Curtis
(Dstl, U.K.)

C. Soutis, Y. Zhuk, I. Guz
(Imperial College of Science, Technology & Medicine, U.K.)

Keywords: *layered structures, impact behaviour, strength, stiffened panels*

Abstract

The in-plane compressive behaviour of thin-skin stiffened composite panels with a stress concentrator in the form of an open hole or low velocity impact damage is examined analytically. A fracture mechanics model, developed initially to predict notched compressive strength, was applied to estimate the compression-after-impact strength of a stiffened panel; in the analysis the impact damage is replaced with an equivalent open hole. The influence of the stiffener on the compressive strength of the thin-skin panel is examined and included in the analysis. A good agreement between experimental measurements and predicted values for the critical failure load is obtained.

1 Introduction

The investigation of compressive behaviour of stiffened thin-skinned composite panels with a stress concentrators is dictated by the demands of aircraft industry. A typical aircraft structure such as a fuselage shell or a wing surface usually consists of a thin skin reinforced with stiffeners. The need for an open cut-out in a subcomponent is required by practical concerns. For example, cut-outs in wing spars and cover panels of commercial and military transport wings are needed to provide access for hydraulic and electrical lines and for damage inspection. Also, cut-outs in a fuselage can serve as access panels and lightening holes. However, such cut-outs introduce high local stresses in the structure that can initiate damage and premature failures. Low velocity impact damage caused by dropped tools, runway debris and hailstones can be another source of stress concentration and therefore weakening of the structure. During a component's service life, it will experience compressive loads and its strength becomes an important design parameter, since compressive strength of currently used carbon fibre-epoxy composites is only 60-70% of their tensile strength. In some applications, these structural elements are required primarily to resist buckling, and in other cases they must carry load well into the post-buckling range in order to yield weight savings. Thus, understanding their buckling and post-buckling behaviour is needed for their design.

In recent years, most of the research has focused on the buckling and post-buckling response of stiffened panels where failure occurs due to large out-of-plane deflections (more than twice the skin thickness) at compressive loads far below the ultimate static strength of the composite material. A comprehensive review of experimental studies of buckling and post-buckling behaviour of laminated composite plates with cut-outs was given in [5]. Later the influence of stiffeners on behaviour of damaged and undamaged plates was experimentally studied in [3]. The effect of stiffeners on the stress distribution around a hole, as well as on buckling and failure

characteristics of lightweight composite panels is the subject of the survey [4].

2 Failure mechanisms

Recent works [7-9] have examined the influence of single and multiple holes on the compressive behaviour of several T800/924C carbon fibre-epoxy laminates without stiffeners. They found that open holes reduce the in-plane compressive strength by more than 40% depending on lay-up and hole size. Damage is initiated by 0º fibre microbuckling at the edge of the hole at approximately 80% of the failure load, and is accompanied by matrix cracking of the off-axis plies and delamination between the plies. This damage zone continues to grow, first in short discrete increments and then rapidly across the laminate width at a failure load that is higher than that predicted by the maximum stress criterion. Fibre buckling leads to local delamination when the local strain necessary to accommodate the localised fibre displacement and rotation exceeds the resin ductility. These local delaminations do not propagate to become macroscopic delaminations until final compressive failure occurs. For 0° dominated laminates, the damage zone is more crack-like in nature and its length immediately prior to failure is in the region of 2-3*mm* long.

A similar damage pattern was observed in stiffened composite plates with impact damage under uniaxial compression [8]. The distribution of damage through-the-thickness determined from sectioning studies is roughly cylindrical in shape; ultrasonic C-scan images and X-ray shadow radiographs indicate that the shape of the overall damage is approximately circular (equivalent to an open hole). Because of this resemblance, a fracture mechanics model [7,9], developed initially to describe this damage sequence in notched composite laminates, is applied below to estimate the compression-after-impact strength of a stiffened panel. In the analysis the impact damage is replaced with an equivalent open hole.

In the present work an effort is made to be as close to actual geometry, lay-up and material properties as possible. All these parameters are taken from a recent experimental investigation funded by the aircraft industry [1]. The general configuration of the panel examined is sketched in Figure 1. It is assumed that the hole or equivalent hole that represents impact damage is always located in the middle of the bay, a more critical situation for thin skins [3]. Three different configurations with an elliptical hole are analysed and the geometrical parameters are presented in Table 1.

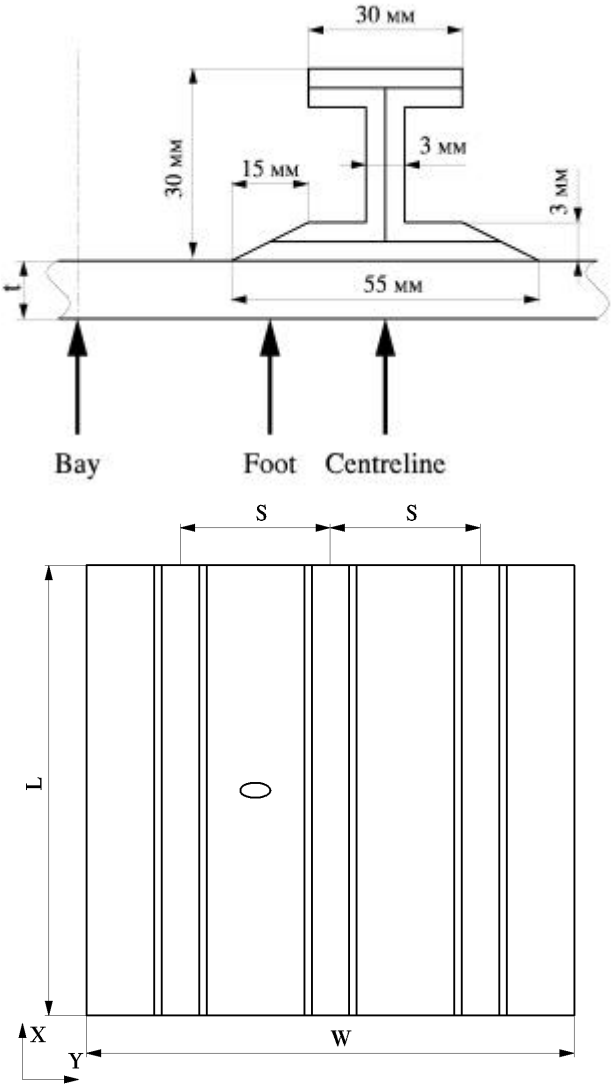

Figure 1. Geometry of the stiffened panel [1].

Table 1. Dimensions of the stiffened panels

Panel	*t, mm*	*S, mm*	W, *mm*	$e_{buckling}$, *me*
Type 1	4	120	360	6000
Type 2	4	148	444	3700
Type 3	3	120	360	3700

Each panel is made of a quasi-isotropic skin with a $[45°/-45°/0°/90°]_{4s}$ lay-up. Fibredux T800/924 (Toray 800 fibres in Ciba Fibredux 924 epoxy resin) was used as a material for each layer. The I-section stiffener is fabricated from four uncured laminates, consisting of a base, two C-sections placed back-to-back and a spar cap. The base and the C-sections have the same lay-up $[+45°/-45°/0°]_{2S}$ whilst that of the spar cap is $[-45°/+45°/0°]_{2S}$; the material used is also T800/924 carbon fibre-epoxy system. The properties of the unidirectional composite pre-preg used are given in [1]. Each of these panels is subjected to uniaxial compression in the direction of the stiffeners.

3 Description of the Soutis-Fleck fracture model and the associated FE analyses

In this section, the Soutis-Fleck fracture model [7,9] is briefly explained. The original model considers a multi-directional composite laminate with an open hole subjected to uniaxial compression. Failure of such laminates is mainly due to 0° fibre buckling from the hole edges, accompanied by fibre/matrix debonding, matrix yielding and delamination. Due to its crack-like appearance the damage zone is mathematically replaced with a line-crack with no traction on its surfaces. The model is based on the following two criteria:

i) Stable crack growth: It is postulated that microbuckling occurs over a distance l from the hole along the transverse *y*-axis when the average stress over this distance reaches the critical stress of the unnotched laminate, s_{un},

$$s_{un} = \frac{1}{l}\int_{R}^{R+l} s_{xx}(0,y)\,dy \qquad (1)$$

For a stiffened panel with a hole of radius *R* loaded along the *x*-axis, the stress distribution $s_{xx}(0,y)$ is found using the finite element method. After numerical integration, the remote applied stress (s^{∞}_{xx}) is obtained as a function of the undamaged strength s_{un}, hole radius *R* and damage length *l*

$$s^{\infty}_{xx} = s_{un} \times f(R,l,A_{ij}), \qquad (2)$$

where A_{ij} is the extensional stiffness matrix of the laminate.

Experimental evidence [7,8] shows that in unnotched multidirectional laminates loaded in compression failure is always by 0° fibre microbuckling and the failure strain is almost independent of lay-up and comparable to the failure strain of the unidirectional laminate. Therefore, by using the laminate plate theory, the unnotched strength, s_{un}, can be replaced in equation (2) by the unidirectional strength, s^{0}_{c}, i.e.,

$$s^{\infty}_{xx} = s^{0}_{c}\, g(R,l,E,l) \qquad (3)$$

where *g* is a function of the hole radius *R*, the crack length *l*, the laminate and 0° lamina stiffness properties *E*.

ii) Unstable crack growth: The microbuckled zone at the edge of the hole is assumed to behave as a crack of the same length, with no traction on the crack surfaces. Then the stress intensity factor (SIF) at the tip of the crack is expressed as

$$K_I = s^{\infty}_{xx}\sqrt{p(R+l)}\,Y(R,l,A_{ij}), \qquad (4)$$

where *Y* is a function of geometry and orthotropy, which can be obtained numerically. The model assumes that unstable crack growth occurs when the SIF at the crack tip is equal to the laminate in-plane fracture toughness K_{IC} and, therefore,

$$s^{\infty}_{xx} = \frac{K_{IC}}{\sqrt{p(R+l)}\,Y(R,l,A_{ij})}, \qquad (5)$$

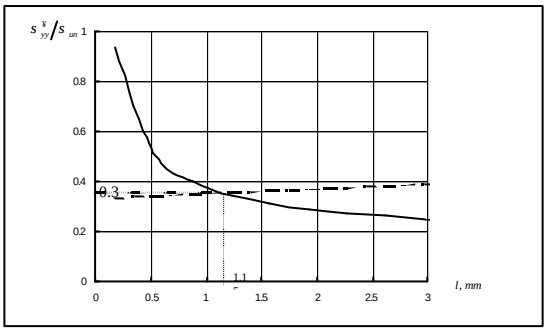

Figure 2. An example of calculating the stable and unstable crack growth.

An example of calculating the stable and unstable crack growth is given in Figure 2 (by the hatched and solid lines, respectively) for type 1 stiffened panel. Total width of the plate is W=240mm, dimensions of elliptical hole are $2a$=56.9mm and $2b$=49.5mm, the layers are fabricated from T800/924 with the lay-up $[(45/-45/0/90)_4]_S$. Using Eqs. (23) and (25), s^{∞}_{xx} is plotted as a function of damage length l. Then the failure strength of the skin of the stiffened panel with a hole and the critical microbuckling length are obtained from the point where the two curves intersect. Coupon tests [9] were used to measure both the unnotched strength and the 'compressive' toughness of the laminated skin, which are required as the model input. For the T800/924C quasi-isotropic lay-up, s_{un}=596MPa and K_{IC}=42 $MPa\sqrt{m}$.

Over the last twenty years or so, the finite element method (FEM) has become firmly established as a standard procedure for deriving stress distributions or values of SIFs in notched composite laminates or structures [11]. To determine the SIF given by Eq. (24) the main essence of the procedure lies in the J-integral evaluation over a predetermined area that includes the crack. In the present work, the FE77 [2] was used and the change of strain energy dU of the whole plate with a differential crack advance dl was calculated. The J-integral is the negative 1st derivative of the strain energy with respect to crack extension. For an elastic body, J is identical to the elastic strain energy release rate G,

$$G = J = -\frac{\partial U}{\partial l} \qquad (6)$$

A rather refined mesh was used to provide reliable results. Orthotropic quadrilateral eight node elements were chosen for the mesh. In general, more coarse mesh can be considered because of the integral nature of energy. For an orthotropic laminate the energy release rate G is related to the SIF, K_I , by

$$G = cK_I^2, \qquad (7)$$

where for plane stress loading, c is the laminate compliance obtained from the following expression

$$c = \left(\frac{a_{11}a_{22}}{2}\right)^{1/2}\left[\left(\frac{a_{22}}{a_{11}}\right)^{1/2} + \frac{2a_{12}+a_{33}}{2a_{11}}\right]^{1/2} \qquad (8)$$

with

$$[a] = \begin{bmatrix} \frac{1}{E_1} & -\frac{n_{21}}{E_2} & 0 \\ -\frac{n_{12}}{E_1} & \frac{1}{E_2} & 0 \\ 0 & 0 & \frac{1}{G_{12}} \end{bmatrix} \qquad (9)$$

Here E and G are the laminate extensional and shear moduli respectively, and n is the Poisson's ratio; 1 is the loading axis (x-axis) and 2 is the transverse direction (y-axis).

In order to investigate the accuracy of the finite element model the SIF for a quasi-isotropic lay-up $[45°/-45°/0°/90°]_{3s}$ obtained numerically is compared to the analytical solution for an isotropic material. The close-form solution for plate with circular hole is given by [7,9]

$$K_I = s^{\infty}\sqrt{p\,d}\,F_1F_2 \qquad (10)$$

where F_1 is the circular hole correction factor

$$F_1 = f\sqrt{1-\frac{R}{d}}, \quad d = R + l \qquad (11)$$

The function f for two symmetric cracks emanating from a circular hole according to [6], is

$$f = 1 + 0.35\,l + 1.425\,l^2 - 1.578\,l^3 + 2.156\,l$$

where

$$l = R/d \qquad (12)$$

The quantity F_2 is a FWC factor [7,9] and is equal to

$$F_2 = \sqrt{\sec\left(\frac{p\,R}{2W}\right)\sec\left(\frac{p\,d}{2W}\right)} \qquad (13)$$

Finite element and analytical results for the plate without stiffeners of a total width W=240mm, length L=712mm and hole radius R=14mm are compared in Figure 3. The dashed and dotted lines correspond respectively to the closed form solutions with and without the finite width correction factor. FEM predictions are in a very good agreement with theory; the difference between the two approaches is less than 2%, giving confidence to the FE analysis and mesh used.

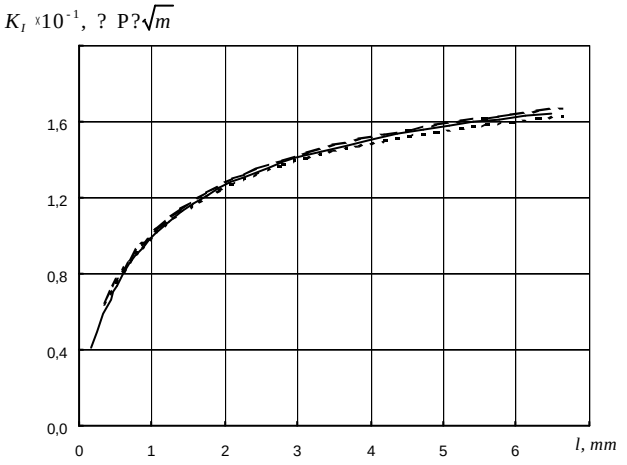

Figure 3. Verification of the FE procedure: SIFs for the case of a circular hole with two cracks.

4 Numerical results

The same procedure was followed for the SIF calculation for a stiffened panel containing an elliptical cut-out. The accuracy of the FE model was confirmed by comparing results to the analytical solution [10] for the case of an elliptical hole. Comparisons for the hole with half-axes a =16.9mm, b=13.3mm are shown in Figure 4 for the same material of layers and layup as in Figure 3. The dotted line corresponds to the analytical solution and the solid line gives the FEM prediction. Some discrepancy for small crack length is due to the error induced by mesh refinement.

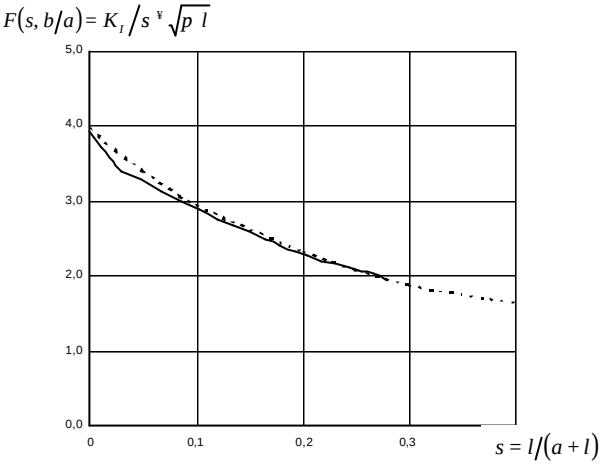

Figure 4. SIFs for the case of an elliptical hole with two cracks.

Then the three panel configurations described in section 2 were analysed. The dimensions of the elliptical holes simulating low velocity impact damage are: $2a = 56.9\,mm$, $2b = 49.5\,mm$ (panel type 1); $2a = 33.8\,mm$, $2b = 26.6\,mm$ (panel type 2); $2a = 27.5\,mm$, $2b = 27.7\,mm$ (panel type 3).

SIFs for the panels with a cracked elliptical hole are plotted in Figure 5 for the three panels (lines 1, 2 and 3, respectively). In the analysis, in order to reduce the calculation effort, only a segment of the panel (W=240mm) is examined. It contains the cracked hole and two adjacent stiffeners. It should be noted that the elliptical hole with half-axes $a = 13.75\,mm$ and $b = 13.85\,mm$ is almost a circular hole with radius $R = 14\,mm$ (SIF for this case is shown in Figure 4 by the line 4).

Once the stress distributions and the SIFs are known, the Soutis-Fleck fracture model [7-9] can be applied to estimate the critical compressive load of the stiffened panel with an open hole or impact damage that is replaced with an equivalent hole. Following the procedure described in section 3, the ratio s_{xx}/s_{un} in this case for panel type 1 is given by equations (3) and (5) and plotted versus crack

length l, Figure 2. Then the failure stress of the laminate as well as the critical buckled length l_{cr} is obtained from the point where the two curves intersect. The calculated critical loads and their deviation from experimental data [1] are shown in Table 2. The theoretical values are close to measurements for panels 1 and 3 (difference <4%). The model underestimates the failure load for panel type 2 by ~26%, suggesting that the effect of the impact damage is not as severe as that of an open hole. A region with reduced stiffness properties (a soft inclusion) could give a better approximation than using an open hole in the model.

One more reason for the deviation between the experimental and predicted values for the critical load for the plate type 2 can be given. The panels were reported [1] to be designed to buckle at a certain compressive strains ($e_{buckling}$ in Table 1). It is clear (Table 3) that panels type 1 and type 3 have failed before out-of-plane buckling started, meanwhile panel type 2 failed after this type of buckling occurred. However, the equivalent crack model is designed to predict failure due to in-plane fibres buckling (kinking) and, therefore, gives lower prediction for critical load in case when out-of-plane buckling mechanism becomes dominating.

It should also be said that the scatter in the measurement of material constants (s_{un}, K_{IC}) could introduce additional errors.

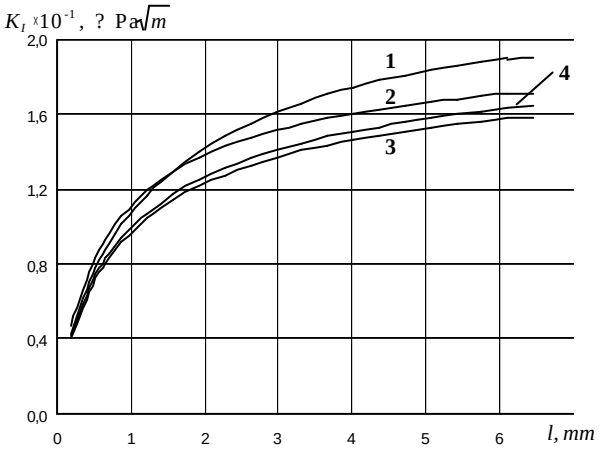

Figure 5. SIFs for three stiffened panels with a cracked open hole determined numerically.

Table 2. Failure loads and critical stress results; s_{un} = 596 *MPa* , (·) experimental value.

Panel type	l_{cr}, *mm*	s_{xxcr}/s_{un}	P_{cr}^{th}, *kN*	Deviation from experimental results
1	1.15	0.351	-511.0 (-529)	-3.4%
2	1.35	0.324	-538.0 (-734)	-26%
3	1.39	0.372	-456.5 (-460)	<-1%

Table 3. The experimental and predicted values for the critical load (in μe).

Panel type	1	2	3
Experimental strain at failure [1]	–3262	–4543	–3597
Analytical prediction	–3443	–3179	–3649
Design buckling strain [1]	–6000	–3700	–3700
Experimental buckling strain [1]	–	–4400	–3600

5 Conclusions

The influence of the stiffener on the compressive strength of the stiffened panel was examined and included in the analysis. In the range of the model applicability critical loads predicted by the model are close to measured data.

Further work is needed to predict compressive strength of stiffened composite panels with a stress concentrator in case of out-of-plane buckling. In this case failure mechanism is different from those discussed above. Therefore, a comprehensive fracture analysis of stiffened composite panels should consist of two stages. In the first, one should perform the in-plane fracture analysis described in this work and the second stage should be devoted to obtain the load when out-of-plane buckling generates fracture. The minimum of these two loads should be taken as the design fracture load (critical load) of the given panel. In future work, the compressive failure of a stiffened panel with a stress raiser due to out-of-plane buckling will be examined.

Acknowledgement

This work was carried out with the support of the UK MoD.

References

[1] Greenhalgh E, Singh S, Hughes D and Roberts D. Impact damage resistance tolerance of stringer stiffened composite structures. *Plastics, Rubber and Composites*. Vol. 28, No. 5, pp 228–251, 1999.

[2] Hitchings D. *FE77 Users Manual*. Imperial College, Aeronautics, 1995.

[3] Jegley DC. Effect of low-speed impact damage and damage location on behavior of composite panels. *NASA Technical Paper 3196*, 1992.

[4] Liessa AW. An overview of composite plate buckling. *Composite Structures 4, Analyses and Design Studies*, Vol. 1 (ed.: IM Marshall), Elsevier, pp 1.1–1.29, 1987.

[5] Nemeth MP. Buckling and post buckling behavior of laminated composite plates with a cut-out. *NASA Technical Paper 3587*, 1996.

[6] Newman JC. A nonlinear fracture mechanics approach to the growth of small cracks. *Proc AGARD Conference "Behaviour of Short Cracks on Airframe Components"*, France, 1982.

[7] Soutis C. Damage tolerance of open-hole CFRP laminates loaded in compression. *Composite Engineering*., Vol. 4, No. 3, pp 317–327, 1994.

[8] Soutis C and Curtis P. Prediction of the post-impact compressive strength of CFRP laminated composites. *Composite Science and Technology*, Vol. 56, No. 6, pp 677–684, 1996.

[9] Soutis C and Fleck N. Static compression failure of carbon fibre T800/924C composite plate with a single hole. *Journal of Composite Materials*, Vol. 24, No. 5, pp 536–558, 1990.

[10] Tada H. *The Stress Analysis of Cracks.* Del Research Corporation, 1974.

[11] Tan SC. *Stress Concentrations in Laminated Composites*. Technomic Publishing, 1994.